⌘ *Author's Choice*

THE JOURNAL OF BIOLOGICAL CHEMISTRY VOL. 286, NO. 1, pp. 441–449, January 7, 2011

Biochemical and Structural Studies of a HECT-like Ubiquitin Ligase from *Escherichia coli* O157:H7*

Received for publication, July 23, 2010, and in revised form, September 28, 2010 Published, JBC Papers in Press, October 27, 2010, DOI 10.1074/jbc.M110.167643

David Yin-wei Lin[‡], Jianbo Diao[§], Daoguo Zhou[‡], and Jue Chen[‡¶1]

From the [‡]Department of Biological Sciences, Purdue University and [¶]Howard Hughes Medical Institute, West Lafayette, Indiana 47907 and the [§]Institutes of Biomedical Sciences, Fudan University, Shanghai 200032, China

Many microbial pathogens deliver effector proteins via the type III secretion system into infected host cells. Elucidating the function of these effectors is essential for our understanding of pathogenesis. Here, we describe biochemical and structural characterization of an effector protein (NleL) from *Escherichia coli* O157:H7, a widespread pathogen causing severe foodborne diseases. We show that NleL functionally and structurally mimics eukaryotic HECT E3 ligases and catalyzes formation of unanchored polyubiquitin chains using Lys^6 and Lys^{48} linkage. The catalytic cysteine residue forms a thioester intermediate with ubiquitin. The structure of NleL contains two domains, a β-helix domain formed by pentapeptide repeats and a bilobed catalytic domain reminiscent of the N- and C-lobe architecture of HECT E3s. Six structures of NleL observed in two crystal forms revealed a large range of different positions of the C-lobe relative to the N-lobe, indicating that the helix linking the two lobes is extremely flexible. Comparing the structure of NleL with that of the *Salmonella* homolog SopA showed that the orientation of the C-lobes differ by as much as 108°, suggesting that large movements of the C-lobe may be required to facilitate the transfer of ubiquitin from E2 to the substrate. These results provide critical knowledge toward understanding the molecular mechanism by which pathogens utilize the host ubiquitination system during infection.

In eukaryotes, ubiquitination plays important roles in many cellular functions, including protein degradation, DNA repair, cell-cycle progression, trafficking, and endocytosis (1). The event of ubiquitination involves a multienzyme cascade consisting of classes of enzymes known as ubiquitin-activating enzymes (E1), conjugating enzymes (E2), and ligases (E3). The E1 enzyme activates a free ubiquitin (Ub)[2] by forming a thioester bond between its active site cysteine and the carboxyl terminus of Ub using the energy from ATP hydrolysis; the activated Ub is then passed to the active cysteine on the E2 conjugating enzyme; finally, E3 mediates the transfer of the Ub from E2 to the substrate (2, 3). The E3 ligases are particularly important in conferring substrate specificity by interacting directly with the target proteins. There are two major E3 families: the RING (really interesting new gene) finger (2) and the HECT (homologous to E6AP carboxyl terminus) (3, 4). RING and HECT E3s function through very different mechanisms. RING E3s catalyze ubiquitination by serving as a molecular scaffold to bring the Ub-charged E2 and the substrate into close proximity, whereas HECT E3s directly participate in the chemistry by forming a thioester bond with the Ub molecule brought by E2 and then direct it to the substrate protein. Crystal structures of the catalytic domain of HECT E3s (5–8) show a common fold of two lobes (the N- and C-lobes) linked by a flexible loop. Structural and mutagenesis studies (5) suggest that the conformational flexibility of the HECT domain is important for transferring Ub from E2 to the substrate.

Although the ubiquitination pathway is absent in bacteria, some pathogenic bacteria deliver effector proteins into eukaryotic host cells to function as E3 ligases (9–13). For example, AvrPtoB from *Pseudomonas syringae* contains a RING finger/U-box-like domain and ubiquitinates a tomato kinase, Fen, to disrupt the plant immunity (14, 15). *Shigella* effector IpaH9.8 catalyzes Ub transfer reactions through an active site cysteine (16–19). A homologous protein of IpaH in *Salmonella*, SspHI, targets host cell protein PKN1 kinase for degradation (20, 21). Recently, we also reported that SopA from *Salmonella* is an E3 ligase structurally similar to eukaryotic HECT E3s (22, 23).

In this study, we biochemically and structurally characterized NleL (non-Lee-encoded effector ligase), a homologue of SopA from *Escherichia coli* O157:H7. Previously, it was shown that NleL (named EspX7) was an effector protein translocated into host cell via the type III secretion system (24, 25). But little has been known about the function of NleL in host cells. Here, we show that NleL catalyzes formation of unanchored polyubiquitin chain using Lys^6 and Lys^{48} linkage. Similar to SopA, the structure of NleL contains a β-helix domain and a catalytic domain with a bilobed fold. The relative orientations between the two lobes revealed in the structures of NleL and SopA are markedly different, suggesting that like eukaryotic HECT E3s, the flexibility of the C-lobe is essential in Ub transfer.

EXPERIMENTAL PROCEDURES

Protein Expression and Purification—The gene encoding NleL was amplified from the genomic DNA of *E. coli O157:H7*

* This work was supported by Howard Hughes Medical Institute.

The atomic coordinates and structure factors (codes 3NB2 and 3NAW) have been deposited in the Protein Data Bank, Research Collaboratory for Structural Bioinformatics, Rutgers University, New Brunswick, NJ (http://www.rcsb.org/).

⌘ *Author's Choice*—Final version full access.

[1] A Howard Hughes Medical Institute investigator. To whom correspondence should be addressed. E-mail: chenjue@purdue.edu.

[2] The abbreviations used are: Ub, ubiquitin; polyUb, polyubiquitin; MES, 4-morpholineethanesulfonic acid; NEL, novel E3 ligase.

str. Sakai and subcloned into a pMCSG20 plasmid containing an N-terminal GST tag. Point mutations were generated using the QuikChange site-directed mutagenesis kit (Stratagene). The plasmid containing $NleL^{170-782}$ was transformed into *E. coli* strain BL21-CodonPlus (DE3)-RIL (Stratagene). Bacteria were grown to log phase in LB medium at 37 °C, and protein expression was induced with 0.1 mM isopropyl 1-thio-β-D-galactopyranoside at 16 °C for 24 h. GST-$NleL^{170-782}$ was purified by glutathione Sepharose affinity chromatography followed by tobacco etch virus protease digestion to remove the GST tag. $NleL^{170-782}$ was further purified by gel filtration (Superdex 200, GE Healthcare) and ion exchange (SOURCE 15Q, GE Healthcare) chromatography. Selenomethionine-substituted protein was prepared as the native protein except that bacterial cells were grown in M9 minimal media supplemented with glucose, vitamins, and amino acids with L-methionine replaced by L-selenomethionine (Molecular Dimensions).

Ubiquitination Assays—Ubiquitination reactions of NleL were performed in 50-μl reaction mixtures containing 50 mM Tris-HCl, pH 7.5, 50 mM NaCl, 2 mM ATP, 5 mM $MgCl_2$, 0.1–0.2 mM DTT, 20 μg of Ub, 0.1 μg of E1, 0.25 μg of E2, and 5 μg of $NleL^{170-782}$. Reactions were incubated at 25 °C for 30 min unless indicated otherwise and terminated by the addition of SDS-PAGE sample buffer. Ubiquitination reactions for the Ub linkage preference were performed with 0.25 μg of E1 instead for 1 h. Thioester formation experiments were performed on ice with 1 μg of E1, 10 μg of E2, and 10 μg of $NleL^{170-782}$ in the presence of 1 mM DTT. Oxyester formation experiments of $NleL^{170-782}$ C753S were done at 25 °C with the same amount of proteins as the thioester formation experiments. Recombinant E1, UbcH5a, UbcH7, and wild-type Ub proteins were prepared following published protocols (22, 26). Other E2 enzymes and mutant Ubs were purchased from Boston Biochem. Anti-Ub and anti-GST antibodies were purchased from Santa Cruz Biotechnology; anti-UbcH7 antibody was purchased from BD Biosciences. Rabbit polyclonal anti-NleL antibody was produced by ProSci against purified $NleL^{170-782}$.

Crystallography—The protein sample was concentrated to 25 mg/ml in a buffer containing 10 mM Tris, pH 8.0, and 5 mM DTT and crystallized by the sitting drop vapor diffusion method at 20 °C by mixing 0.2 μl of protein with 0.1 μl of reservoir solution containing 0.1 M MES, pH 6.0, 1.0 M Li_2SO_4, and 16% glycerol. Crystals were flash frozen in liquid nitrogen with the reservoir solution before mounting. Diffraction data were collected at 100 K on beam line 23-ID at the Advanced Photon Source (The General Medicine and Cancer Institutes Collaborative Access Team, Argonne National Laboratory) and processed with HKL2000 (27). Using diffraction data between 50–2.5 Å, 46 of 48 sites of selenium atoms from two NleL molecules were located by SOLVE (28). The experimental phase was improved by density modification using the program RESOLVE (29). The model was built by automated model building in RESOLVE (30) and followed by manually building using Coot (31). Refinement was performed in CNS (32) and Phenix (33). The partially refined selenomethionine-substituted structure was used as a molecular replacement

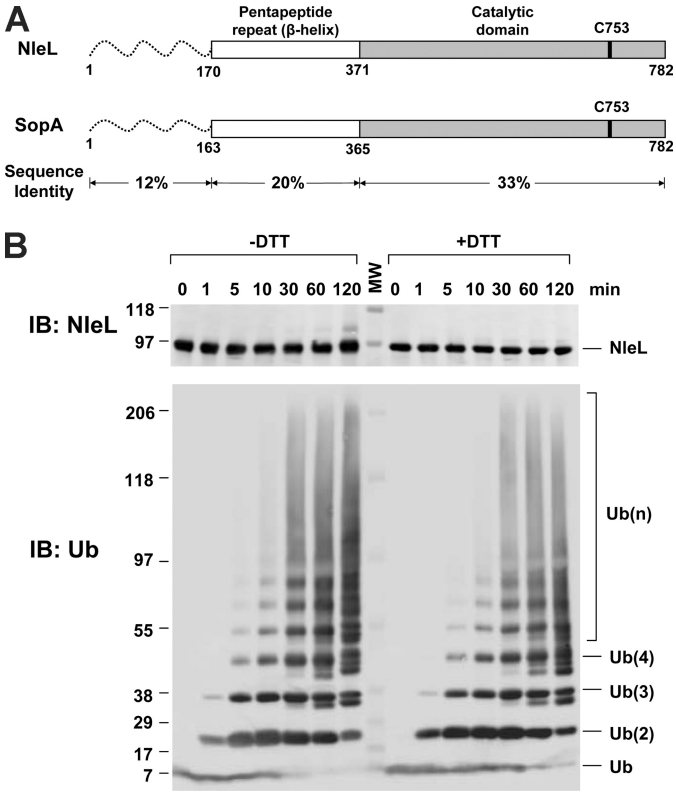

FIGURE 1. **NleL is an E3 ligase that assembles free polyubiquitin chain.** *A*, schematic representation of NleL in comparison to SopA. *B*, ubiquitin ligase activity of NleL. $NleL^{170-782}$ was incubated with ATP, Ub, E1, and E2 (UbcH7) at room temperature for indicated times. The reaction mixture was loaded onto SDS-PAGE in the absence or presence of DTT, visualized by immunoblotting using antibodies against NleL (*upper panel*) and ubiquitin (Ub) (*lower panel*). *IB*, immunoblot; *MW*, molecular mass marker. The positions of the molecular mass markers are indicated in kDa.

model to phase the structure of the native protein, consisting of four NleL molecules per asymmetric unit, using PHASER (34). The final native NleL structure was refined to 2.1 Å with R and R_{free} factors of 18.3 and 23.1%. The stereochemistry of the structure was checked by PROCHECK in the CCP4 program suite (35) with 99.9% of the residues in the most favored and additional allowed regions, 0.1% in the generously allowed region, and none in the disallowed region on the Ramachandran plot (Table 1). All structural figures were prepared using PyMOL (36).

RESULTS

NleL Assembles Unanchored Polyubiquitin Chain—NleL from *E. coli* O157:H7 shares an overall 26% sequence identity to SopA with a conserved cysteine residue (Cys^{753}) at the active site (Fig. 1*A*). Similar to SopA, limited proteolysis of the full-length protein suggested that the first 169 residues are not structured. Residues 170–370 of NleL contain tandemly repeated amino acid sequences that belong to the pentapeptide repeat protein family (37, 38). The catalytic HECT-like domain is located at the C terminus, which shows the highest sequence similarity to SopA in comparison with the other regions.

A stable construct consisting of residues 170 to 782 ($NleL^{170-782}$) was purified to characterize its ubiquitin ligase

activity. When incubated with purified E1, E2 (UbcH7), Ub, and ATP, $NleL^{170-782}$ catalyzed formation of polyubiquitin (polyUb) chains (Fig. 1*B*). Addition of a reducing reagent DTT did not change the mobility of the polyUb bands on SDS-PAGE, indicating that the polyUb chains were not anchored to another protein through a thioester bond (Fig. 1*B*). Multiple bands with slightly different mobility were observed at positions corresponding to three or more covalently linked Ub molecules (Fig. 1*B*). As the Ub chain can be linked via one of the seven lysine residues, and the chains can be either linear or branched, the heterogeneity observed on SDS-PAGE suggested that NleL might synthesize polyUb chains containing multiple linkage types. Immunoblotting with antibodies against NleL (Fig. 1*B*) or UbcH7 (data not shown) indicated that with wild-type Ub, little autoubiquitination of NleL or ubiquitination of UbcH7 was observed. In contrast, SopA preferentially catalyzes autoubiquitination in the absence of native substrates (22, 23). Therefore, the *in vitro* ligase activities of the two homologous ligases appear to be different.

Catalytic Cysteine Residue Forms a Thioester Intermediate—Both SopA and NleL contain a cysteine residue near the C terminus (Cys^{753} in both proteins), at a position similar to that of the catalytic cysteine in eukaryotic HECT E3s. Mutation of Cys^{753} to serine was shown to abolish the autoubiquitination activity of SopA (22, 23). Similarly, the C753S mutation in NleL lowers its activity compared with wild-type protein (Fig. 2*A*). Specifically, under conditions in which the polyUb chain was readily formed by wild-type NleL, only a small amount of $Ub_{(2)}$, $Ub_{(3)}$, and $Ub_{(4)}$ were observed with the C753S mutant. When Cys^{753} was replaced with alanine, little Ub chain formation was observed.

To test whether Cys^{753} of NleL forms a transient thioester bond with Ub, two noncatalytic cysteine residues, 17 and 137, of E2 were mutated to serine to avoid nonspecific cross-linking in the absence of reducing reagents. UbcH7 (C17S, C137S) was incubated with Ub, E1, and ATP until almost all E2 molecules were charged with Ub (Fig. 2*B*, *lane 1*). NleL was then added to the reaction mixture, and the products were analyzed in the absence and presence of 100 mM DTT (Fig. 2*B*). Several DTT-sensitive bands, corresponding to the molecular weights of NleL linked with single and multiple Ubs, were detected when the catalytic cysteine is intact. Mutating the active site Cys^{753} to serine or alanine abolished the formation of thioester intermediates (Fig. 2*B*, *lanes 6* and *7*). Instead, with the C753S mutant, DTT-resistant NleL~$Ub_{(n)}$ slowly built up after 10 min of incubation (Fig. 2*C*). Precharged E2~Ub was hydrolyzed much slower by the C753S mutant in comparison with the wild-type NleL (Fig. 2, *B* and *C*, *lower panels*). These data suggest that the serine residue at the active site forms an oxyester bond with Ub, a linkage more stable than a thioester bond.

The presence of NleL~$Ub_{(n)}$ products in the nonreducing gel indicates that more than one Ub molecule was assembled on Cys^{753} via a thioester linkage. Because only mono-Ub-charged E2 was detected (Fig. 2, *B* and *C*, *lane 1*), it is unlikely that the polyUb chain was preassembled on E2 as observed for Ube2g2/gp78 (39). The other possibility is that polyUb chains synthesized and released from E3 were conjugated back to the catalytic site. In that case, one would expect accumulation of NleL~$Ub_{(n)}$ with time as more polyUb chains are synthesized. However, the kinetics of the reaction was the opposite; the amount of the NleL~$Ub_{(n)}$ intermediates decreased rapidly with time; after 30 s, only monoubiquitinated NleL was observed (Fig. 2*B*, *lane 5*). Thus, it seems more likely that NleL catalyzes chain formation by a sequential model (40, 41). In a normal turnover, the acceptor Ub binds noncovalently to NleL, and a chain is synthesized by the addition of Ub one at a time (Fig. 2*D*). When pulsed with charged E2, the acceptor Ub could be conjugated to E3 through the thioester bond because E3~Ub was abundant, and a chain was built up at the active site (Fig. 2*E*). As the reaction progressed, and the amount of charged E2 and E3 returned to the steady state, the E3~$Ub_{(n)}$ product became undetectable by immunoblotting, as shown in Fig. 2*B*.

NleL Interacts with E2s Containing a Conserved Phenylalanine—To analyze the E2 preference of NleL, assays were conducted using nine different human E2s, among which six supported the formation of polyUb chains (Fig. 3*A*). The E2 preference of NleL overlaps with that of SopA (22) and is consistent with that of eukaryotic HECT E3s. Eukaryotic HECT E3s work with E2s that contain a conserved phenylalanine residue (Phe^{63} in UbcH7) (8, 42). Among the 9 E2s tested, an equivalent phenylalanine residue is conserved in all E2s that function with NleL but not in those that do not support ubiquitination (Fig. 3*B*). Thus, similar to eukaryotic HECT E3s, both NleL and SopA interact with E2 through its conserved phenylalanine residue.

NleL Catalyzes Formation of Lys^{6}- and Lys^{48}-linked Chains—Because different linkages of Ub may signal different cellular processes, Ub mutants were used to study the nature of the isopeptide linkage catalyzed by NleL. Using mutants containing no or only one of the seven lysine residues (single Lys Ub), little polyUb chain formation was observed except when lysine was present at position 6 or 48 (mutants K6 and K48) (Fig. 4*A*). Interestingly, whereas the autoubiquitination activity is very low with wild-type Ub (WT) and the K6 and K48 mutants, mono- and diubiquitinated NleL products were prominent with mutants that do not support free polyUb chain formation (Fig. 4*A*). Ubiquitination of UbcH7 was also observed with mutants other than K6 and K48 (Fig. 4*A*). Using mutant Ub where only one of the seven lysine residues was substituted by arginine (single KR mutant), polyUb chain formation but little autoubiquitination was observed (Fig. 4*B*). These results indicate that NleL preferentially catalyzes free polyUb chain formation through both Lys^{6} and Lys^{48} linkages. In the absence of Lys^{6} and Lys^{48}, both NleL and E2 can be subjected to ubiquitination through all other possible isopeptide linkages. The chain type specificity of NleL is independent of E2, as identical results were obtained with three different E2s tested (UbcH2, UbcH5a, and UbcH7). Because the experiments were carried out without the authentic substrate, it is possible that in the host cell, NleL builds Lys^{6}- and/or Lys^{48}-linked Ub chains on the substrate instead of catalyzing the formation of free polyUb chains.

Structure of NleL Is Similar to That of SopA—Crystals of $NleL^{170-782}$ were obtained in two different forms, both be-

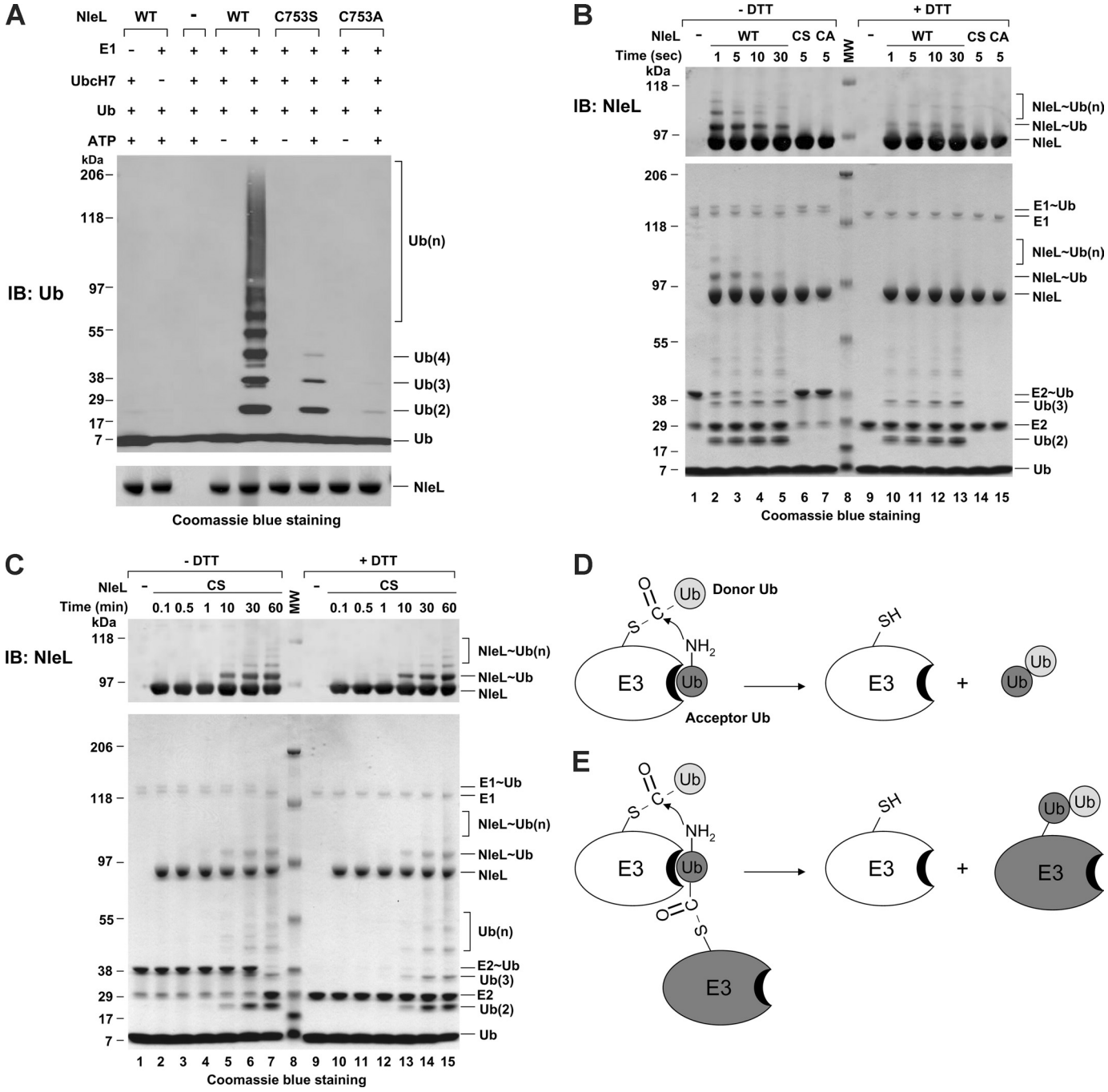

FIGURE 2. **Cysteine 753 is required for the HECT-like ligase activity.** *A*, WT and two mutant NleL$^{170-782}$ (C753S and C753A) were incubated with E1, E2 (UbcH7), Ub, and ATP at room temperature for 30 min. The reaction products were analyzed by immunoblotting (*IB*) with an antibody against Ub (*top*) or SDS-PAGE stained with Coomassie Blue (*bottom*). *B*, shown is a thioester formation. UbcH7 (C17S, C137S) mutant was precharged by E1 in the presence of Ub and ATP on ice for 10 min before NleL was added to the mixture. Reactions were quenched at indicated time points by SDS-gel sample loading buffer and analyzed under non-reducing (−DTT) and reducing (+DTT) conditions. *WT*, NleL$^{170-782}$; *CS*, NleL$^{170-782}$ mutant containing C753S; *CA*, NleL$^{170-782}$ mutant containing C753A; *MW*, molecular mass. The small amounts of NleL∼Ub$_{(n)}$ products present in the reducing lanes were due to autoubiquitination. *C*, oxyester formation of NleL (C753S) mutant pulsed with precharged E2 as in *B*. *D*, shown is a potential mechanism for polyUb chain formation catalyzed by NleL, figure modified from Wang and Pickart (40). *E*, the potential mechanism by which NleL∼Ub$_{(n)}$ is synthesized in the E2∼Ub pulse experiment. In this model, as the acceptor ubiquitin is linked to NleL by a thioester (WT) or oxyester (C753S), the chain is built up on the active site of the substrate E3∼Ub.

longing to space group C2 (Table 1). One crystal form contains four molecules per asymmetric unit and the other contains two. The structure of the crystal containing two molecules per asymmetric unit was determined by multiwavelength anomalous diffraction using a selenomethionine derivative. The structure of the second crystal was determined by molecular replacement using the first structure. Each NleL molecule consists of two parts (Fig. 5*A*): the pentapeptide repeat motif (residues 171–371), which forms a right-handed quadrilateral β-helix; and the C-terminal bilobed structure (residues 372–782) that resembles the N- and C-lobes of eukaryotic HECT E3 ligases (18). The structures of the C-termi-

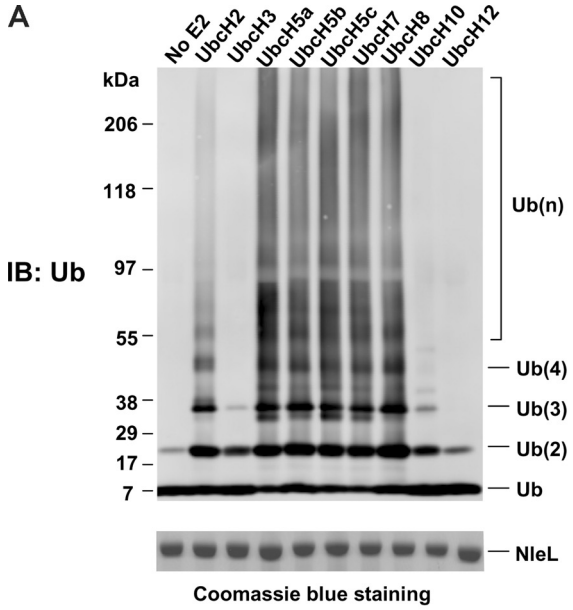

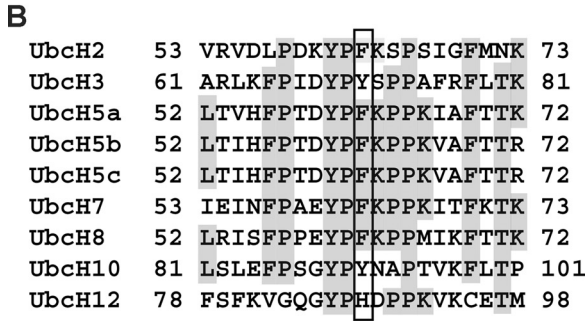

FIGURE 3. **E2 preference.** *A*, *in vitro* ubiquitination assays. NleL$^{170-782}$ was incubated with E1, indicated E2s, Ub, and ATP at room temperature for 30 min and then immunoblotted with an antibody against Ub. The same samples were also analyzed by SDS-PAGE Coomassie Blue staining to show that approximately equal amount of NleL was used in all reactions. *B*, local sequence alignment of all the E2s used in this assay. The *box* indicates Phe^{63} of UbcH7 that is conserved in all E2s supporting the ligase activities of HECT E3s. *IB*, immunoblot.

nal regions are similar in NleL and SopA, with an root mean square deviation of 1.9 Å over 208 Cα atoms in the N-lobe and 1.5 Å over 160 Cα atoms in the C-lobe. However, the relative orientation of the C-lobes is markedly different; the largest angular displacement is 108° between the structures of NleL and SopA (Fig. 5*A*). Consequently, the active site cysteine of NleL points away from the β-helix domain, which is opposite to the orientation in SopA. Consistent with the relatively low sequence identity (20%), the β-helix domains of NleL and SopA have more structural differences than the catalytic domains. The NleL β-helix has an additional coil in the cylindrical structure, whereas the corresponding residues in SopA form less ordered loops (Fig. 5*B*). As the only structured region preceding the catalytic domain, the β-helix domain is likely to be responsible for substrate binding. However, in the absence of knowledge of the targeting substrates, it is difficult to correlate the structural differences with the functional differences between the two ligases.

Conformational Flexibility—Rigid body movement of the C-lobe is a characteristic of HECT E3 ligases. Among the four known structures of eukaryotic HECT domains, the relative orientation of the C-lobe to the N-lobe varies significantly (5–8). The structure of the E6AP-E2 complex provides a clear hint that rotation of the C-lobe is necessary for its function; two active cysteine residues located in E2 and E3 are 41 Å apart. For Ub transfer from E2 to E3, the two active sites must be located within 7–8 Å. Mutations that either shorten the hinge loop or reduce its flexibility diminish the catalytic activity, indicating that conformational flexibility within the HECT domain is essential for substrate ubiquitination (5).

In SopA and NleL, the linker between the N- and C-lobes is an α-helix consisting of 23 residues, instead of a short (three or four residues) unstructured loop seen in eukaryotic HECT E3s. Still, SopA also shows rigid body motion of the C lobe. Between the two structures of SopA, the C-lobe rotates ~25° relative to the N-lobe, resulting a displacement of the active

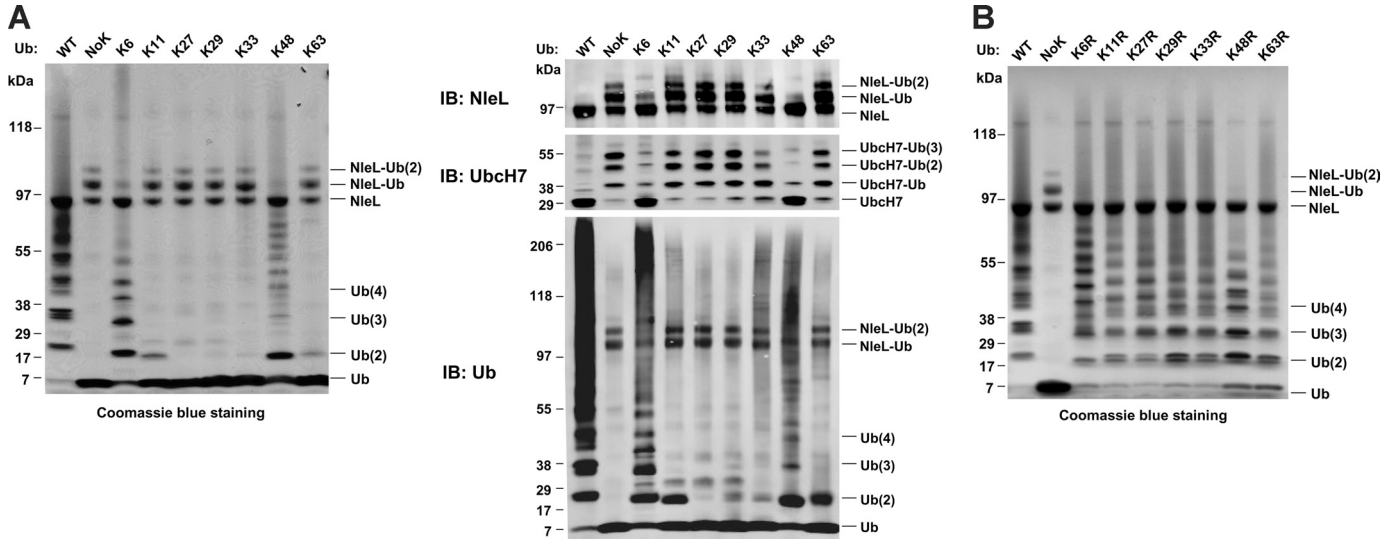

FIGURE 4. **Ubiquitin linkage specificity.** *A*, ubiquitination assay of NleL$^{170-782}$ in the presence of E1, UbcH7, Ub (WT), or the indicated mutants containing a single lysine residue. *NoK*, no lysine residues. Following an incubation of 1 h at room temperature, the products were resolved by SDS-PAGE and visualized by Coomassie staining or by immunoblotting (*IB*) using antibodies against NleL, UbcH7, or Ub. *B*, ubiquitination assays performed with single Lys-to-Arg ubiquitin mutants.

TABLE 1
Crystallographic and Refinement statistics

	Native	Se-Met			
Diffraction Data					
Space group	*C2*	*C2*			
Cell dimensions					
a × *b* × *c* (Å)	177.1×124.2×154.9	313.8×77.3×61.5			
α × β × γ (°)	90×107.6×90	90.0×94.5×90.0			
No. of molecules per A.U.	4	2			
		Remote1	*Peak*	*Inflection*	*Remote2*
Wavelength (Å)	1.07223	1.0115	0.9794	0.9796	0.9494
Resolution range (Å)[1]	44.7-2.1 (2.2-2.1)	50-2.5 (2.6-2.5)	50-2.5 (2.6-2.5)	50-2.5 (2.6-2.5)	50-2.5 (2.6-2.5)
No. of reflections	185858	49257	50366	49831	49783
Completeness (%)[1]	99.7 (100.0)	97.9 (91.1)	98.7 (97.4)	98.7 (97.6)	98.7 (97.8)
R_{sym}[1]	0.072 (0.338)	0.060 (0.044)	0.118 (0.581)	0.104 (0.620)	0.095 (0.626)
$I / \sigma I$ [1]	22.1 (2.6)	16.6 (8.5)	12.6 (3.8)	12.8 (3.4)	12.4 (3.5)
Redundancy[1]	3.8 (3.8)	11.5 (11.0)	7.6 (7.0)	7.6 (7.0)	7.6 (7.2)
Refinement					
R_{work} (%)	18.28	18.27			
R_{free} (%) [2]	23.14	24.81			
No. of atoms					
Protein	19411	9640			
Ligand/ion	330	106			
H_2O	1098	295			
R.m.s. deviations					
Bond length (Å)	0.007	0.008			
Bond angle (°)	1.02	1.08			
B-factors					
Protein	45.5	62.4			
Ligand/Ion	70.7	90.5			
Water	49.4	56.0			
Ramachandran plot					
Allowed (%)	99.9	99.9			
Generously allowed (%)	0.1	0.1			
Disallowed (%)	0	0			

[1] Numbers in brackets refer to the highest resolution shell.
[2] A random 5% of the reflection data was omitted in the refinement and used to calculate R_{free}.

site cysteine by 14 Å (23). Superposition of the six NleL molecules observed in the two crystal forms (Table 1) onto each other reveals that, as in SopA, the relative orientations of the N-lobe and the β-helix domain remain essentially unchanged; however, the positions of C-lobes vary significantly (Fig. 6*A*). The hinge rotation of the C-lobes range from 2–76° among the structures compared. The largest displacement of Cys^{753} between two structures of NleL is 15 Å. Therefore, it seems that the flexibility of the C-lobe is a conserved structural feature of HECT E3s that microbial pathogens have evolved to mimic.

The observed flexibility of the C-lobe is achieved through conformational changes of the hinge helix (residues 593–615). A comparison of the structures of NleL and SopA shows a large range of conformations sampled by the hinge helix (Fig. 6*B*). In both structures of SopA, residues in this region fold into an α-helix with two different tilt angles relative to the N-lobe. In NleL crystals, three different secondary structures were observed: a continuous α-helix, two short α-helices connected by a helix turn, or in the third case, residues at the turn (604–606) form a 3_{10} helix (Fig. 6*B*). It is likely that unique conformations captured in the crystal structures of NleL and SopA are stabilized by crystal lattice forces. Nevertheless, the permitted flexibility undoubtedly reflects a functional requirement that is essential for ligase activity.

Superposition of the six isolated C-lobes reveals four flexible surface regions (Fig. 6*C*). The largest displacement (~12 Å) is observed for residues in the loop preceding the active site. This loop is the only region with limited sequence similarity between bacterial HECT (SopA and NleL) and eukaryotic HECT E3s (23). Mutation of Thr^{752} in SopA reduces the autoubiquitination activity. As residues critically involved in

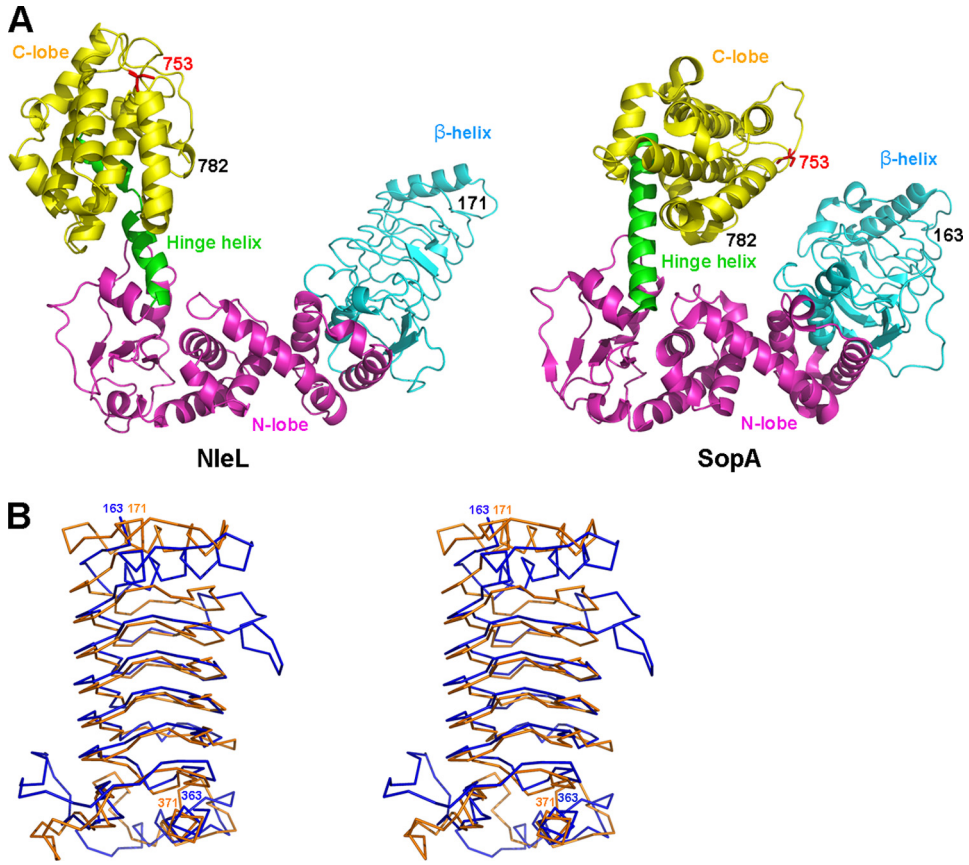

FIGURE 5. **Structure of NleL$^{170-782}$ is similar to that of SopA$^{163-782}$.** *A*, both structures consist of three regions: the β-helix domain (*cyan*), the N-lobe (*magenta*), and the C-lobe (*yellow*). The connecting helices between the two lobes are shown in *green*, and the catalytic cysteines (Cys^{753}) are indicated in *red*. *B*, stereoview of superposition of the β-helix domains from NleL (*yellow*) and SopA (*blue*).

protein/protein or protein/ligand interactions are often mobile in the absence of their binding partners, the observed flexibility of the active-site loop in isolated NleL structures may reflect its function in interacting with other molecules such as E2 or Ub in a transthiolation reaction.

DISCUSSION

Here, we report the biochemical and structural characterization of NleL, a previously uncharacterized T3SS effector protein from enterohemorrhagic *E. coli* O157:H7. Similar to SopA, NleL contains a protease-sensitive N terminus, a β-helix domain, and a C-terminal catalytic domain that resembles the bilobed architecture of eukaryotic HECT E3s. Whereas the N-lobe of NleL is of similar shape and size to that of E6AP, the C-lobes of NleL and E6AP are different in size and fold (8, 23). Unlike eukaryotic HECT, the N- and C- lobes of NleL are connected by a helix; however, the conformational flexibility of the helix functionally mimics that of the unstructured loop in E6AP. Formation of a thioester intermediate is characteristic of HECT E3s. The ubiquitin ligase activity of NleL is dependent upon a cysteine residue (Cys^{753}) that forms an intermediate with Ub through a thioester bond. *In vitro* ubiquitination assay shows that NleL preferably forms unanchored polyUb chains using Lys^{6} and Lys^{48} linkages.

Ubiquitination is absent in bacteria; therefore, it is likely that NleL is synthesized by pathogenic bacteria to function exclusively in eukaryotic hosts. Very often, prokaryotes incorporate eukaryotic genes directly into their genome by a mechanism called horizontal gene transfer (13). However, because NleL shows no sequence homology to any eukaryotic proteins, it seems likely that NleL is acquired through convergent evolution. A BLAST search against all sequenced genomes found homologs of NleL in *Citrobacter rodentium* ICC168, *E. coli* E22, and more than a dozen *Salmonella* strains. A common feature of these bacteria is that they all cause disease in humans and warm-blooded animals. Comparative genomic analysis suggested that *Salmonella* and *E. coli* diverged ~100 million years ago (43) and pathogenic *E. coli* such as enterohemorrhagic *E. coli* separated from nonpathogenic strains around 4.5 million years ago (44). Although one cannot exclude the possibility that *Salmonella* and enterohemorrhagic *E. coli* obtained the genes of SopA and NleL independently, it is more likely that *Salmonella* acquired the HECT-like protein (SopA) during co-evolution with the eukaryotic hosts. Then, this gene was introduced into other pathogenic bacteria such as enterohemorrhagic *E. coli*, enteropathogenic *E. coli*, and *C. rodentium* through lateral gene transfer, a common mechanism for the distribution of genes in the microbial community (13).

In addition to RING or HECT-like E3s, a family of bacterial effector proteins has been recently discovered to have ubiquitin ligase activity without any sequence or structural simi-

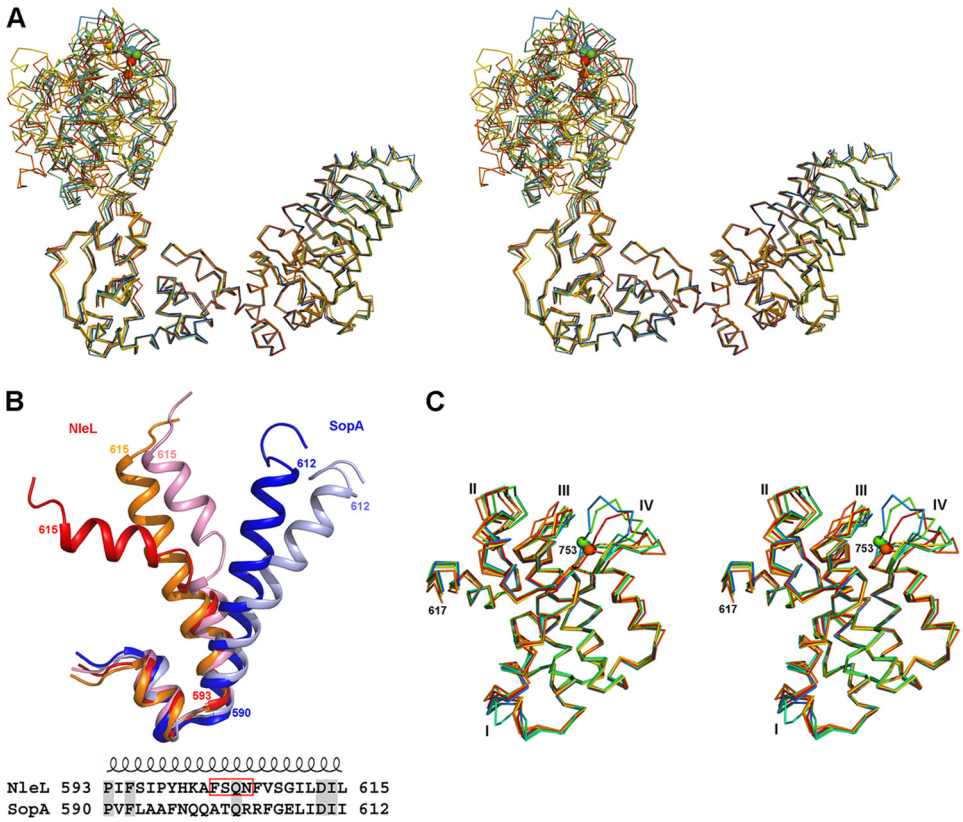

FIGURE 6. **Conformational flexibility observed in NleL and SopA structures.** *A*, stereoview of superposition of the six NleL structures observed in the two crystal forms. The catalytic Cys^{753} is represented as *balls*. *B*, different conformations of the hinge helix. The two structures of SopA (*blue* and *cyan*) and three representative structures of NleL (*orange*, *pink*, and *red*) are superimposed based on the N-lobes and the β-helix domains. The sequences of the NleL and SopA hinge helix are shown with the helix-break residues *boxed*. *C*, stereoview of the superposition of the C-lobe from the six NleL structures, showing conformational flexibility within the C-lobe. The catalytic Cys^{753} residue is represented as a *ball*. Labeled are the four most flexible regions: *I*, residues 637–644; *II*, residues 668–672; *III*, residues 704–708; and *IV*, residues 746–753.

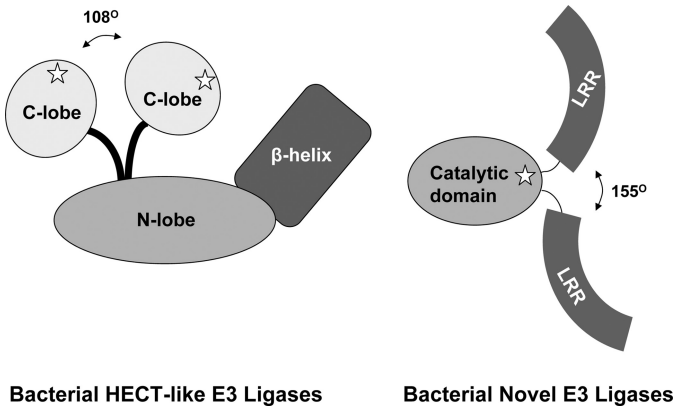

FIGURE 7. **Schematic comparison of two families of bacterial E3 ligases.** *Left*, HECT-like E3 ligases including NleL and SopA, where the relative orientations of the β-helix domains and the N-lobes are fixed, but the C-lobes are flexible. The largest rotation of the C-lobes between the structures of NleL and SopA is 108°. *Right*, the NELs represented by *Shigella* IpaH3 (Protein Data Bank code 3CVR) and *Salmonella* SspH2 (Protein Data Bank code 3G06). Superposition of the catalytic domains of IpaH3 and SspH2 indicates a large hinge rotation of the leucine-rich repeat (*LRR*) domain. The catalytic cysteine residue is indicated by a *star*.

larity to any eukaryotic ligases (10, 16–18, 20). This group of proteins, termed NEL for Novel E3 ligases, contains two structural domains: an N-terminal leucine-rich repeat, which presumably interacts with substrates, and a C-terminal α-helical domain, which accounts for the catalytic activity. A conserved cysteine residue in the catalytic domain also forms a thioester bond with Ub (16, 17); thus, NEL is related to HECT E3s in terms of the chemistry of transthiolation. Structurally, NEL is very different from that of HECT E3 ligases. In contrast to NleL and SopA, where the relative orientation of the β-helical domain and the N-lobe is fixed, two structures of NELs showed marked difference in the relative position of the leucine-rich repeat domains (Fig. 7) (10, 17, 20). Although flexibility is also observed within the catalytic domain of NEL, the extent of its motion is much less than in NleL or SopA (16, 17).

The recent discovery of bacterial effector proteins functioning as ubiquitin ligases opens a new field. Although more than a half dozen of these ligases have been characterized structurally and biochemically, many questions remain unanswered. For example, how did the microbes initially acquire these proteins to function in eukaryotic hosts? Do eukaryotic counterparts of NEL exist? What is the function of these ligases in the life cycle of the bacteria? Investigations into these questions will provide a better understanding of bacterial pathogenesis, evolutionary biology, and the molecular mechanisms of ubiquitination.

Acknowledgments—We thank the staff at the Advanced Photon Source beam line 23-ID for assistance with data collection and Dr. Jon Huibregtse for comments on the manuscript.

REFERENCES

1. Kerscher, O., Felberbaum, R., and Hochstrasser, M. (2006) *Annu. Rev. Cell Dev. Biol.* **22,** 159–180
2. Freemont, P. S. (1993) *Ann. N.Y. Acad. Sci.* **684,** 174–192
3. Huibregtse, J. M., Scheffner, M., Beaudenon, S., and Howley, P. M. (1995) *Proc. Natl. Acad. Sci. U.S.A.* **92,** 5249
4. Pickart, C. M. (2001) *Annu. Rev. Biochem.* **70,** 503–533
5. Verdecia, M. A., Joazeiro, C. A., Wells, N. J., Ferrer, J. L., Bowman, M. E., Hunter, T., and Noel, J. P. (2003) *Mol. Cell* **11,** 249–259
6. Ogunjimi, A. A., Briant, D. J., Pece-Barbara, N., Le Roy, C., Di Guglielmo, G. M., Kavsak, P., Rasmussen, R. K., Seet, B. T., Sicheri, F., and Wrana, J. L. (2005) *Mol. Cell* **19,** 297–308
7. Kamadurai, H. B., Souphron, J., Scott, D. C., Duda, D. M., Miller, D. J., Stringer, D., Piper, R. C., and Schulman, B. A. (2009) *Mol. Cell* **36,** 1095–1102
8. Huang, L., Kinnucan, E., Wang, G., Beaudenon, S., Howley, P. M., Huibregtse, J. M., and Pavletich, N. P. (1999) *Science* **286,** 1321–1326
9. Collins, C. A., and Brown, E. J. (2010) *Trends Cell Biol.* **20,** 205–213
10. Hicks, S. W., and Galán, J. E. (2010) *Curr. Opin. Microbiol.* **13,** 41–46
11. Angot, A., Vergunst, A., Genin, S., and Peeters, N. (2007) *PLoS Pathog.* **3,** e3
12. Munro, P., Flatau, G., and Lemichez, E. (2007) *Curr. Opin. Microbiol.* **10,** 39–46
13. Spallek, T., Robatzek, S., and Göhre, V. (2009) *Cell Microbiol.* **11,** 1425–1434
14. Janjusevic, R., Abramovitch, R. B., Martin, G. B., and Stebbins, C. E. (2006) *Science* **311,** 222–226
15. Rosebrock, T. R., Zeng, L., Brady, J. J., Abramovitch, R. B., Xiao, F., and Martin, G. B. (2007) *Nature* **448,** 370–374
16. Singer, A. U., Rohde, J. R., Lam, R., Skarina, T., Kagan, O., Dileo, R., Chirgadze, N. Y., Cuff, M. E., Joachimiak, A., Tyers, M., Sansonetti, P. J., Parsot, C., and Savchenko, A. (2008) *Nat. Struct. Mol. Biol.* **15,** 1293–1301
17. Zhu, Y., Li, H., Hu, L., Wang, J., Zhou, Y., Pang, Z., Liu, L., and Shao, F. (2008) *Nat. Struct. Mol. Biol.* **15,** 1302–1308
18. Rohde, J. R., Breitkreutz, A., Chenal, A., Sansonetti, P. J., and Parsot, C. (2007) *Cell Host. Microbe.* **1,** 77–83
19. Ashida, H., Kim, M., Schmidt-Supprian, M., Ma, A., Ogawa, M., and Sasakawa, C. (2010) *Nat. Cell Biol.* **12,** 66–73
20. Quezada, C. M., Hicks, S. W., Galán, J. E., and Stebbins, C. E. (2009) *Proc. Natl. Acad. Sci. U.S.A.* **106,** 4864–4869
21. Haraga, A., and Miller, S. I. (2006) *Cell Microbiol.* **8,** 837–846
22. Zhang, Y., Higashide, W. M., McCormick, B. A., Chen, J., and Zhou, D. (2006) *Mol. Microbiol.* **62,** 786–793
23. Diao, J., Zhang, Y., Huibregtse, J. M., Zhou, D., and Chen, J. (2008) *Nat. Struct. Mol. Biol.* **15,** 65–70
24. Tobe, T., Beatson, S. A., Taniguchi, H., Abe, H., Bailey, C. M., Fivian, A., Younis, R., Matthews, S., Marches, O., Frankel, G., Hayashi, T., and Pallen, M. J. (2006) *Proc. Natl. Acad. Sci. U.S.A.* **103,** 14941–14946
25. Deng, W., de Hoog, C. L., Yu, H. B., Li, Y., Croxen, M. A., Thomas, N. A., Puente, J. L., Foster, L. J., and Finlay, B. B. (2010) *J. Biol. Chem.* **285,** 6790–6800
26. Lee, I., and Schindelin, H. (2008) *Cell* **134,** 268–278
27. Otwinowski, Z., and Minor, W. (1997) *Methods Enzymol.* **276,** 307–326
28. Terwilliger, T. C., and Berendzen, J. (1999) *Acta Crystallogr. D. Biol. Crystallogr.* **55,** 849–861
29. Terwilliger, T. C. (2000) *Acta Crystallogr. D. Biol. Crystallogr.* **56,** 965–972
30. Terwilliger, T. C. (2003) *Acta Crystallogr. D. Biol. Crystallogr.* **59,** 38–44
31. Emsley, P., and Cowtan, K. (2004) *Acta Crystallogr. D. Biol. Crystallogr.* **60,** 2126–2132
32. Brünger, A. T., Adams, P. D., Clore, G. M., DeLano, W. L., Gros, P., Grosse-Kunstleve, R. W., Jiang, J. S., Kuszewski, J., Nilges, M., Pannu, N. S., Read, R. J., Rice, L. M., Simonson, T., and Warren, G. L. (1998) *Acta Crystallogr. D. Biol. Crystallogr.* **54,** 905–921
33. Afonine, P. V., Grosse-Kunstleve, R. W., and Adams, P. D. (2005) *Acta Crystallogr. D. Biol. Crystallogr.* **61,** 850–855
34. McCoy, A. J., Grosse-Kunstleve, R. W., Adams, P. D., Winn, M. D., Storoni, L. C., and Read, R. J. (2007) *J. Appl. Crystallogr.* **40,** 658–674
35. Collaborative Computational Project, N. (1994) *Acta Crystallogr. D. Biol. Crystallogr.* **50,** 760–763
36. DeLano, W. L. (2002) *The PyMOL Molecular Graphics System*, DeLano Scientific LLC, San Carlos, CA
37. Bateman, A., Murzin, A. G., and Teichmann, S. A. (1998) *Protein Sci.* **7,** 1477–1480
38. Vetting, M. W., Hegde, S. S., Fajardo, J. E., Fiser, A., Roderick, S. L., Takiff, H. E., and Blanchard, J. S. (2006) *Biochemistry* **45,** 1–10
39. Li, W., Tu, D., Brunger, A. T., and Ye, Y. (2007) *Nature* **446,** 333–337
40. Wang, M., and Pickart, C. M. (2005) *EMBO J.* **24,** 4324–4333
41. Hochstrasser, M. (2006) *Cell* **124,** 27–34
42. Eletr, Z. M., and Kuhlman, B. (2007) *J. Mol. Biol.* **369,** 419–428
43. Porwollik, S., and McClelland, M. (2003) *Microbes. Infect.* **5,** 977–989
44. Reid, S. D., Herbelin, C. J., Bumbaugh, A. C., Selander, R. K., and Whittam, T. S. (2000) *Nature* **406,** 64–67